An asymptotic treatment of the Elenbaas–Heller equation for a radiating wall-stabilized high-pressure gas-discharge arc

An asymptotic treatment of the Elenbaas–Heller equation for a radiating wall-stabilized high-pressure gas-discharge arc

H. K. Kuiken
Philips Research Laboratories, P. O. Box 80 000, 5600 JA Eindhoven, The Netherlands

(Received 28 June 1991; accepted for publication 14 August 1991)

An asymptotic analysis of the Elenbaas–Heller equation for a radiating wall-stabilized high-pressure gas-discharge arc is given. This analysis applies when the operating temperatures within the arc are lower than the ionization temperature by an order of magnitude. It is shown that for arcs that are radiating highly efficiently a further asymptotic treatment can be given. It is shown under what conditions, governed by a dimensionless parameter M, this limiting case prevails. Comparison with earlier results put forward by Zollweg [J. Appl. Phys. **49**, 1077 (1978)] shows satisfactory agreement.

I. INTRODUCTION

In a recent paper[1] we have shown that asymptotic methods can be brought to bear in a study of the classical Elenbaas–Heller (EH) equation for a high-pressure gas discharge. In that preliminary study the arc was assumed to be nonradiating. The present paper will be devoted to the radiating arc. It will be shown that the success of the method extends to this more complicated situation. Indeed, a fully analytical procedure can be set up for arcs that are radiating efficiently, i.e., arcs that convert the larger part of their input power into optically thin radiation. Even when the thermal conductivity is allowed to be a most general function of the temperature, the analytical approach remains effective.

Again, the method is based on the observation that the energy levels related to ionization and radiation are far higher than those within the arc. This results in temperature profiles that are highly concentrated around the axis of the arc. Of course, Elenbaas[2] had already made similar remarks. See, for instance, Fig. 8 of his book on high-pressure mercury discharges. However, Elenbaas assumed a greatly simplified temperature profile. Later authors,[3–7] in attempting to improve upon Elenbaas's work, but still following an analytical course of action, devised all manner of approximations of the highly nonlinear terms that appear in the EH equation. One of these approaches concerns the so-called two-channel model, in which all radiation and heat dissipation are assumed to occur within a narrow channel around the axis. The corresponding nonlinear terms are replaced by linear ones. Outside this narrow channel the EH equation reduces to a simple heat-conduction equation. The trouble with this approach is, of course, that there is no reasonable way of determining where the "interface" between the two regions is located.

With the advent of large-scale computing, interest in the analytical approach, limited in its scope as it had proved itself to be, faded rapidly and, subsequently, the EH equation was solved numerically. Now, even an equation as apparently simple as the EH equation represents a series of physical phenomena, and each of these is characterized by one or more physical parameters. It is inherent to the numerical approach that each of these physical parameters must be assigned definite values before the program can be run. When the parameter set is large, it will be difficult to interpret results in terms of the input parameter values. But then, for design purposes, a clear understanding of how the input values affect the end result is of great importance. If a problem can be solved analytically, there will be a much greater understanding on this score. Therefore, one should always try to carry the analytical approach as far as one is capable of doing. Even if the end result is not as accurate as one would wish, if it is in analytical form, one can use it as a means of spotting trends and may succeed in delimiting the parameter-value set that is most likely to yield results that are feasible from an applications point of view. The numerical software may then be invoked in order to take the final steps towards an accurate end result.

We intend to show in this paper that the analytical aim set out in the previous paragraph can indeed be achieved, giving full credit to all salient nonlinear features of the EH equation. It has frequently been shown before, and will be confirmed again here, that parameter settings that are logical from a technological point of view are often such that asymptotic approaches can be invoked. The rewards are given in the form of explicit expressions linking input and output variables.

II. MODEL

The Elenbaas–Heller equation is defined as follows:

$$\frac{1}{r}\frac{d}{dr}r\lambda(t)\frac{dt}{dr}+\sigma(t)E^2-u(t)=0. \tag{1}$$

The three terms of this equation represent heat conduction, Joule heating, and radiation losses, respectively. The temperature is denoted by t and the temperature-dependent thermal conductivity by $\lambda(t)$. Furthermore, $\sigma(t)$ is the (temperature dependent) electrical conductivity and E is the electric-field strength, which is assumed uniform. Finally, $u(t)$ represents the sum of all optically thin radiation-loss effects. We shall consider a rotationally symmetric situation with r denoting the radial coordinate. The arc is enclosed by a tube with an inner radius given by a. In Eq.

 0021-8979/91/105282-10$03.00

(1) we use a single temperature t, since we assume local thermodynamic equilibrium (LTE) conditions to prevail.

The field E is related to the total current I flowing through the arc:

$$E=I\left(\int_0^a 2\pi\ r\sigma(t)dr\right)^{-1}. \tag{2}$$

The electrical conductivity, which appears in Eqs. (1) and (2), is a function of the temperature and related to Saha's equation

$$\sigma(t)=\gamma t^{3/4}\exp(-t_i/t), \tag{3}$$

where

$$t_i=eV_i/2k, \tag{4}$$

which is equal to half the ionization temperature which, in turn, is related to the ionization energy eV_i, where V_i is the ionization potential and e is the elementary charge. In addition, k is Boltzmann's constant and γ is another constant.

In principle, the radiation processes are very complicated. A full description of these would lead to a very intricate model. In Eq. (1) it is assumed that the radiation process is composed of two extreme types: (i) optically thin radiation as expressed by the energy-loss term $-u(t)$; (ii) optically thick radiation, which is represented by an enhanced thermal conductivity $\lambda(t)$. The analysis that follows is independent of the precise functional description of $\lambda(t)$. The thermal conductivity can be given as an explicit analytical function, which may be quite general, or, alternatively, as a tabulated function in the required temperature range. We write, generally,

$$\lambda=\lambda_r\Lambda(t/t_r), \tag{5}$$

where Λ is a dimensionless function with

$$\Lambda(1)=1. \tag{6}$$

Also, t_r is the temperature on the axis of the tube and λ_r the corresponding thermal conductivity. Clearly, when t_r changes, the definition of Λ changes as well.

Thin radiation constitutes the actual performance of the lamp. In principle, it concerns all lines which radiate visible and invisible light. Referring to Ref. 2, we write

$$u(t)=\sum_j b_j\exp(-t_j/t), \tag{7}$$

where

$$t_j=eV_j/k, \tag{8}$$

eV_j being the excitation energy of the jth line. The coefficients b_j are factors that determine the weight of the line. These factors can be functions of the temperature. Elenbaas[2] suggests that for many practical purposes the series (7) can be replaced by a single term

$$u(t)=b_*\exp(-t_*/t), \tag{9}$$

where t_* is a representative radiation temperature and b_* the corresponding weight factor. In this paper we shall assume that

$$b_*=\omega t^p, \tag{10}$$

so that

$$u(t)=\omega t^p\exp(-t_*/t), \tag{11}$$

where ω is a constant. For monoatomic gases we have $p=-1$. Clearly, an equation such as Eq. (11) is strongly empirical, so that it will be difficult to assign values to both ω and t_* on the basis of pure physical reasoning. Later in this paper we shall resort to curve fitting by demanding that Eq. (11) represent known values reported in the literature. The same will be done for the parameters γ and t_i defined by Eq. (3). It will be shown that this curve fitting can be done quite accurately.

It would seem that Eq. (1), together with Eqs. (2), (3), (5), and (11), is too complicated for analytical treatment and that a numerical approach should be opted for. However, in an earlier paper dealing with a somewhat simpler problem, we showed that an asymptotic approach based on a suitable dimensional analysis may lead to analytical results. The key to the success of that approach is the nondimensionalization of the temperature by means of the axis temperature t_r. Thus, we write

$$t=t_rT \quad \text{and} \quad r=aR, \tag{12}$$

where T and R are dimensionless variables. Substituting these expressions in Eq. (1) and using Eqs. (2), (3), (5), and (11), we find

$$\frac{1}{R}\frac{d}{dR}\Lambda(T)\frac{dT}{dR}+HT^{3/4}\exp\left[T_i\left(1-\frac{1}{T}\right)\right]$$

$$-KT^p\exp\left[T_*\left(1-\frac{1}{T}\right)\right]=0. \tag{13}$$

In Eq. (13) we have

$$H=\alpha f(T_i), \tag{14}$$

where

$$\alpha=I^2/4\pi^2a^2\gamma\lambda_r t_r^{7/4} \tag{15}$$

and

$$f(T_i)=e^{T_i}\left[\int_0^1 RT^{3/4}\exp\left[T_i\left(1-\frac{1}{T}\right)\right]dR\right]^{-2}, \tag{16}$$

with

$$T_i=t_i/t_r \quad \text{and} \quad T_*=t_*/t_r. \tag{17}$$

In Eq. (13) we also have

$$K=\omega t_r^{p-1}a^2\lambda_r^{-1}e^{-T_*}. \tag{18}$$

In addition, there are the boundary conditions

$$R=0: \quad T=1, \ dT/dR=0, \tag{19}$$

$$R=1: \quad T=T_w, \tag{20}$$

where

$$T_w=t_w/t_r. \tag{21}$$

in which t_w is the temperature on the inner tube wall. As in Ref. 1, we seem to have one boundary condition too many (three instead of two) for a differential equation of the second order. However, this has to do with the fact that we took the axis temperature t_r for a known parameter. Therefore, we are no longer allowed to prescribe the arc current I. As a result, the parameter α [Eq. (15)], and, therefore, H [Eq. (14)], are unknown. This is why we need an additional boundary condition in order to be able to determine H in Eq. (13).

III. ASYMPTOTICS FOR LARGE VALUES OF T_i

Equation (13), with four dimensionless parameters, viz. H, K, T_i, and T_*, together with the boundary conditions (19) and (20) which contain a fifth parameter T_w, reduces the problem to its barest essentials. If no further analytical advance were possible, this would be the stage to bring to bear the numerics, not earlier. The reason is that the dimensionless model is well balanced. The results can be plotted against the smallest parameter set. However, further analytical progress is possible, since some important parameters are always extreme, that is to say, for those cases that have practical relevance. Of course, one is free to enter any parameter values into the dimensionless model, but the only reason why we study this model is that it has some bearing on a practical issue, and this practical situation leads invariably to extreme values of some of the pertinent parameters.

We have seen before[1] that T_i has a large value for high-pressure gas discharges. Referring to Eqs. (4) and (17), we conclude that T_i is the ratio of half the ionization temperature and the maximum temperature within the arc. With an ionization potential $V_i \sim 10.7$ V, a value typical for a mercury discharge, we find $t_i \sim 60\,000$ K. Temperatures within mercury discharges are usually not higher than 6000 K, showing that T_i has a value of around 10. The same is true for T_*, since t_* and t_i are in the same temperature range. For some gases t_* is slightly lower than t_i, for most gases it is somewhat larger. Note that $t_* = eV_*/k$, and compare with Eq. (4).

We shall now proceed in the manner explained in Ref. 1. First we write

$$Q = T_i \int_T^1 \Lambda(\rho)\, d\rho, \tag{22}$$

defining a function Q which henceforth replaces the temperature T. The transformation (22) dates back to the last century and, apart from the multiplicative factor T_i, is called the Kirchhoff transformation. Alternatively, Q/T_i is sometimes called the heat-flux potential. It can be seen from Eq. (22) that $Q = 0$ when $T = 1$ on the axis of symmetry. When T drops below unity, the value of the integral increases, and that of Q rises rapidly. At the other end of the interval ($R = 1$), the integral attains a value which is of order unity, showing that Q is large there. This is the basis of the asymptotic approach.

Expanding the integral of Eq. (22) for values of T not too different from unity, we find [since $\Lambda(1) = 1$]

$$Q \sim T_i[(1 - T) + O(1 - T)^2]. \tag{23}$$

Inverting Eq. (23), we obtain

$$T \sim 1 - Q/T_i + O(1/T_i^2). \tag{24}$$

Substituting Eq. (22) in Eq. (13), and using the expanded version of Eq. (23) in the exponential terms, we arrive at the asymptotic form of the EH equation:

$$\frac{1}{Z}\frac{d}{dZ} Z \frac{dQ}{dZ} = e^{-Q} - \xi e^{-\eta Q}, \tag{25}$$

where we have introduced the transformed independent variable

$$Z = R(HT_i)^{1/2}. \tag{26}$$

Terms which tend to zero when $T_i \to \infty$ have been disregarded in Eq. (25). On the basis of what we found in Ref. 1, we can expect Z to assume a very large value at $R = 1$, which is equal to $(HT_i)^{1/2}$.

There are only two parameters left in Eq. (25), viz.

$$\xi = K/H \tag{27}$$

and

$$\eta = T_*/T_i = 2V_*/V_i. \tag{28}$$

The boundary conditions on $Z = 0$ read

$$Q = 0 \quad \text{and} \quad \frac{dQ}{dZ} = 0. \tag{29}$$

We also have

$$Q = Q_w = T_i \int_{T_w}^1 \Lambda(\rho)\, d\rho, \quad \text{at } Z = (HT_i)^{1/2}. \tag{30}$$

Let us now recapitulate what the asymptotics have been able to do for us so far. The heart of the problem is given by the differential equation (25), together with three boundary conditions defined by Eqs. (29) and (30). This system contains only four parameters, viz. ξ and η and the two parameter groups of Eq. (30). However, for each given parameter set (ξ,η) the two initial conditions of Eq. (29) suffice for the definition of all possible solutions Q. Since ξ is not known *a priori*, as it contains the unknown parameter H, condition (30) is needed to fix its value. Clearly, having been able to reduce the parameter set this far, we are in a much better position to present a clear picture of the solution set.

The physical meaning of the parameters ξ and η deserves some discussion. From Eq. (25) it should be clear that ξ somehow determines the relative importance of radiation losses versus power input. It can be deduced that the value of ξ must lie in the interval

$$0 \leqslant \xi \leqslant 1. \tag{31}$$

Indeed, if ξ were larger than unity, an area around the axis would experience a heat sink, which is unphysical. It is obvious from Eq. (28) that η fixes the relative position of the effective radiation level with respect to the ionization level. In Eq. (28) the occurrence of the factor 2 should be noted. The value of η is always smaller than 2. Should the

value of η be much less than unity, the asymptotics will fail, since it is based on the rapid decay of exponential functions. However, this situation will rarely occur in practice.

Equation (25) and its solutions that satisfy the two boundary conditions of Eq. (29) make up the basic structure of our title problem. In an asymptotic sense (T_i large) all possible temperature profiles can be deduced from this basic two-parameter set of solutions. For a given gas mixture the parameter η is fixed and all we have to do is evaluate the solution for various values of ξ. The precise value of ξ is then obtained from an iterative process that will be discussed presently.

IV. SOLUTION

To fix the value of ξ we must first determine the behavior of Q for $Z\to\infty$, so as to be able to apply condition (30). Integrating Eq. (25) twice and applying the two boundary conditions of Eq. (29), we arrive at

$$Q\sim g_1(\xi,\eta)\ln Z - g_2(\xi,\eta), \tag{32}$$

with

$$g_1(\xi,\eta)\sim \int_0^\infty \rho(e^{-Q(\rho)} - \xi e^{-\eta Q(\rho)})d\rho \tag{33}$$

and

$$g_2(\xi,\eta)\sim \int_0^\infty \rho\ln\rho(e^{-Q(\rho)} - \xi e^{-\eta Q(\rho)})d\rho, \tag{34}$$

assuming a parameter set (ξ,η) for which both Eq. (33) and (34) exist. It has been shown in Ref. 1 that Eqs. (32)–(34) exist for $\eta = 1$. For other values of η the integrals have to be evaluated numerically. The numerics show that Eqs. (33) and (34) always exist when $\eta\geqslant 1$ and $\xi\leqslant 1$. When $\eta < 1$, the behavior of Q for large Z may differ from that given by Eq. (32). Indeed, the second exponential decays more slowly than the first, so that when $Q\to\infty$ the right-hand side of Eq. (25) always becomes negative beyond a given value of Q defined by

$$Q > Q_{\text{trans}} = [1/(1-\eta)]\ln(1/\xi) \quad (0<\xi,0<\eta<1). \tag{35}$$

We shall not consider this case in the present paper and assume henceforth

$$1\leqslant\eta\leqslant 2. \tag{36}$$

Substituting Eq. (30) in Eq. (32) we find

$$Q_w = T_i\int_{T_w}^1 \Lambda(\rho)d\rho \sim \tfrac{1}{2}g_1\ln(HT_i) - g_2. \tag{37}$$

Since [see Eqs. (16), (24), and (26)]

$$f(T_i)\sim e^{T_i}(HT_i)^2/g_3^2, \tag{38}$$

we find from Eq. (14)

$$H\sim\alpha e^{T_i}(HT_i)^2/g_3^2, \tag{39}$$

where

$$g_3(\xi,\eta) = \int_0^\infty \rho e^{-Q(\rho)}d\rho. \tag{40}$$

Eliminating H between Eqs. (37) and (39) we obtain

$$\alpha\sim(g_3^2/T_i)\exp[-T_i - 2(Q_w+g_2)/g_1], \tag{41}$$

giving the current parameter α [see Eq. (15)] as a function of ξ and η and, of course, T_i and T_w. Similarly, we derive from Eqs. (18), (27), and (37),

$$\xi\sim\Omega\exp[-\eta T_i - 2(Q_w+g_2)/g_1], \tag{42}$$

where

$$\Omega = \omega t_r^{p-2}a^2\lambda_r^{-1}t_i. \tag{43}$$

The solution procedure is now as follows. Since the temperature on the axis is given, the parameters T_i, T_w, and Ω have known values. Furthermore, η has a value fixed by the gas mixture under consideration. Of course, ξ is unknown beforehand, and we intend to determine its value by iteration. In the first step we assume $\xi = 0$. We can now integrate Eq. (25) numerically, using the conditions (29), although for $\xi = 0$ an analytical solution exists (see Ref. 1). The integration process yields values for the parameter functions g_1, g_2, and g_3. The values of g_1 and g_2 are substituted in Eq. (42), yielding a new value of ξ. This new value is used to integrate Eq. (25) anew. This process is continued until convergence is achieved.

When Ω is too large, the new value of ξ may be larger than unity, which we cannot allow. When this occurs, a numerical device called under-relaxation has to be invoked. Choosing a relaxation factor ν between zero and unity, we write

$$\xi_{\text{next}} = \nu\xi_{\text{new}} + (1-\nu)\xi_{\text{old}}. \tag{44}$$

The larger the value of Ω, the smaller we must choose the value of ν. It is found that this invariably forces convergence.

Once a final value of ξ has been reached, we can evaluate Eq. (41) and find the current parameter α which, upon the application of Eq. (15), yields the arc current,

$$I = 2\pi\gamma^{1/2}\lambda_r\omega^{-1/2}t_r^{19/8-p/2}t_i^{-1}\xi^{1/2}g_3(\xi)\exp\left(\frac{t_*-t_i}{2t_r}\right). \tag{45}$$

Similarly, we can find an expression for the field

$$E = \gamma^{-1/2}\omega^{1/2}t_r^{p/2-3/8}\xi^{-1/2}\exp[(t_i-t_*)/2t_r)]. \tag{46}$$

The total power dissipated within the tube is therefore

$$P = 2\pi\lambda_r t_r^2 t_i^{-1}g_3(\xi)l, \tag{47}$$

where l is the effective length of the tube.

To conclude this section we give graphical representations of the functions g_1, g_2, and g_3 in Figs. 1, 2, and 3. These may be used to carry out a quick iteration by hand. In a software implementation one might store the values of g_1, g_2, and g_3 in tabular form in a computer memory, defining particular values by interpolation. This will result in an extremely fast computerized iteration process.

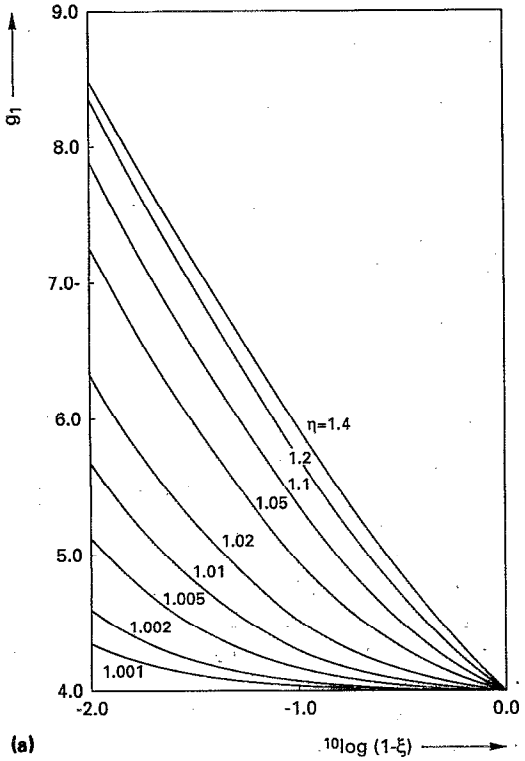

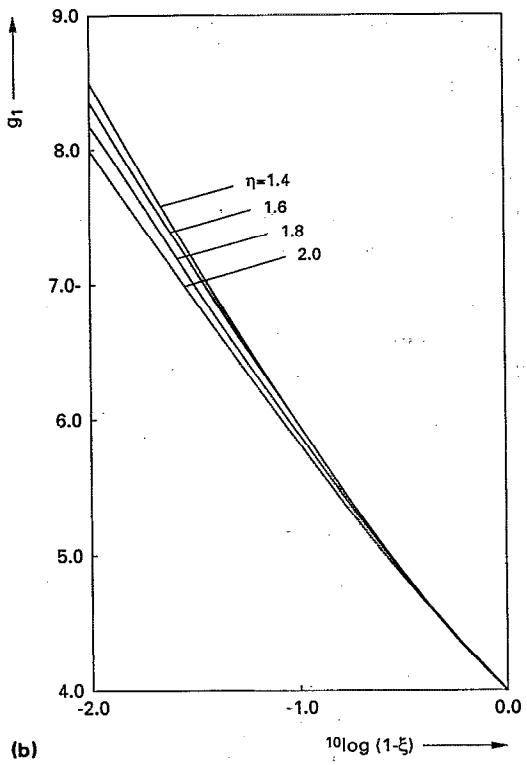

FIG. 1. (a) The function $g_1(\xi)$ which is defined by Eq. (32) and which is used in Eqs. (41) and (42) ($\eta<1.4$). (b) The function $g_1(\xi)$ which is defined by Eq. (32) and which is used in Eqs. (41) and (42) ($\eta>1.4$).

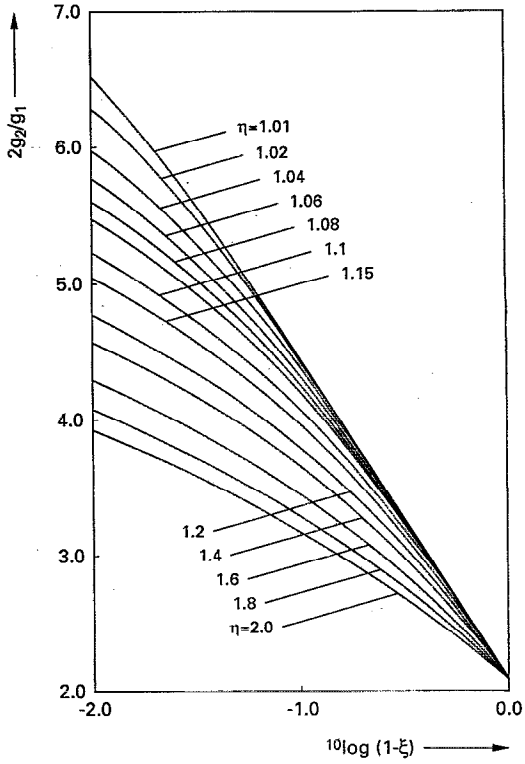

FIG. 2. The function $2g_2(\xi)/g_1(\xi)$ which is defined by Eq. (32) and which is used in Eqs. (41) and (42).

V. RADIATION EFFICIENCY

An important quantity resulting from a realistic lamp model is the radiation efficiency, which is defined by

$$W=\int_0^a ru(t)dr\left(\int_0^a r\sigma(t)E^2dr\right)^{-1}. \tag{48}$$

Equation (48) is the ratio of the power leaving the lamp through radiation and the electric power pumped into it. Going through the various definitions and nondimensionalizations, we may write this asymptotically as

$$W=\xi\int_0^\infty \rho e^{-\eta Q(\rho)}d\rho\left(\int_0^\infty \rho e^{-Q(\rho)}d\rho\right)^{-1}. \tag{49}$$

In general, this quantity will have to be evaluated numerically. In Fig. 4, W is given as a function of ξ for various values of η. Obviously, W has a value between zero and unity. It is interesting to note that, for most values of η, the parameter W reaches values that come near to unity only if ξ comes very close to unity. Since a high radiation efficiency is desirable, this is a first indication that values of ξ close to unity are needed.

VI. COMPARISON WITH RESULTS OBTAINED BY ZOLLWEG

Zollweg[8] calculated and discussed temperature distributions in vertical high-pressure mercury arcs by means of a software package developed by Lowke.[9] This software package includes convection effects. In some of Zollweg's

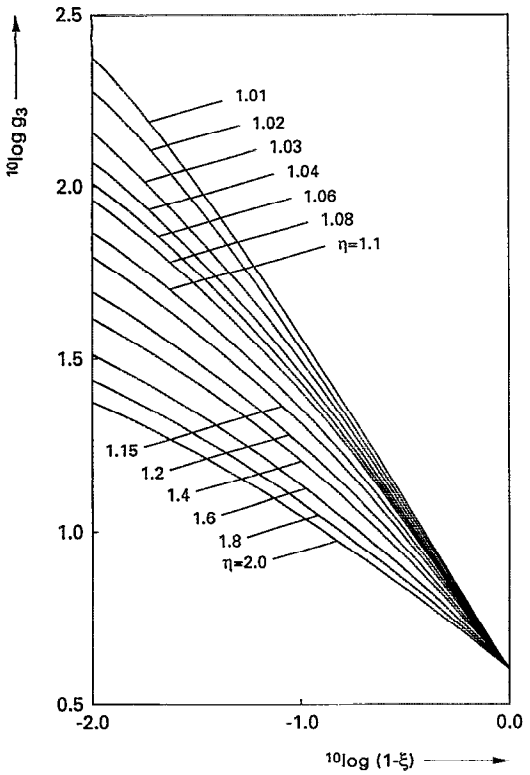

FIG. 3. The function $g_3(\xi)$ which is defined by Eq. (40) and which is used in Eq. (41).

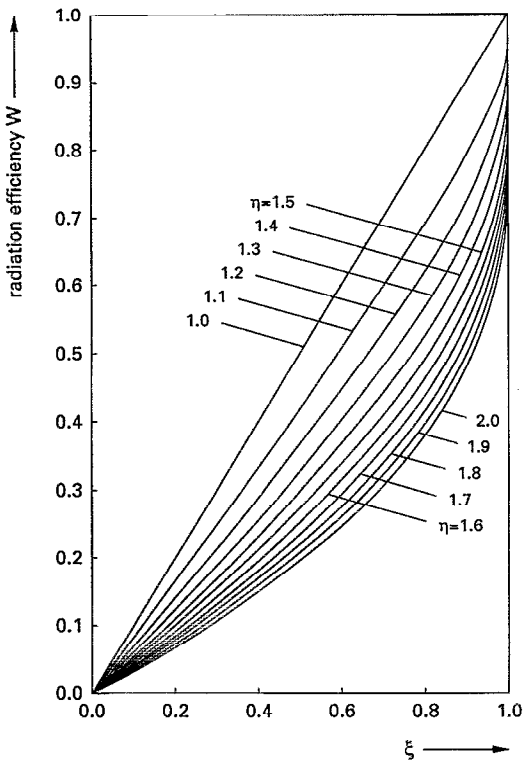

FIG. 4. Radiation efficiency W as defined by Eq. (48).

TABLE I. Comparison of $u(t)$ as given by Zollweg's Table II, last column,[a] and present equation (51). Values reduced to units (W/cm^2 sr) used by Zollweg.

Temperature (K)	Zollweg	$u(t)10^{-6}/4\pi$
7000	112.3	112.3
6500	46.72	47.01
6000	15.76	16.91
5500	5.093	5.013
5000	1.353	1.154
4500	0.1979	0.1897
4000	−0.1605	0.0196
3500	−0.1605	0.0010

[a]See Ref. 8.

numerical experiments, particularly the ones with large mercury charges, convection was seen to influence the temperature fields to some extent. Therefore, a full comparison with Zollweg's results is not possible. Another difference between Zollweg's model and ours is that Zollweg models the energy absorption by means of a negative net emission coefficient, which we do not.

We refer to one of the cases discussed by Zollweg that was least affected by convection. His results were tabulated in his Tables II and V. Zollweg considers a tube with an inner radius of 9 mm and electrode distance of 8 cm. His case I refers to a mercury charge of 51.5 mg, a pressure of 2.89×10^5 N/m^2, a power of 380 W, and a current of 3.0 A. Zollweg lists the gas properties of this case in his Table II. We have found that the electrical conductivity can be modeled by

$$\sigma(t)=1.2\times10^3 t^{3/4}\exp(-54\,600/t)\ \text{(mho/m)}, \qquad (50)$$

and the radiative emission function by

$$u(t)=2.14\times10^{18}t^{-1}\exp(-86\,000/t)\ \text{(W/m}^3\text{)}, \qquad (51)$$

which shows that $t_i=54\,600$ K and $t_*=86\,000$ K, so that $\eta=1.575$. Equation (50) approximates Zollweg's values extremely well. A similar agreement was found in Ref. 10, where we compared an equation such as Eq. (50) with another of Zollweg's cases. The agreement of (51) with Zollweg's results is also quite remarkable (see Table I),

TABLE II. Comparison of radial temperature profiles. Zollweg's values[a] reported in his Table V at axial position $z=4$ cm are shown in the second column. Our results are in column three. The first column gives the radial distance in millimeters.

r	Zollweg	This work
0	5841	5621
1	5802	5605
2	5669	5541
3	5381	5381
4	4883	5053
5	4259	4546
6	3596	3846
7	2899	3063
8	2113	2161
9	1001	1000

[a]See Ref. 8.

except in the lower temperature range ($t<4000$ K), where Zollweg invokes his negative radiative emission model. We also used the thermal conductivity as tabulated by Zollweg. No attempt was made to model these values by an analytical function. As we said before, this is not necessary. All we have to do is rescale the values of Zollweg's table in accordance with Eq. (5), defining the function $\Lambda(T)$, and evaluate Q_w as defined by Eq. (30).

In our model we assume the axis temperature to be known, and then we derive the main lamp functions such as the current and the power. In order to be able to compare our results with Zollweg's, we have chosen a value of t_r that results in a lamp power of 380 W, which is the value quoted by Zollweg. We then find a current of 3.43 A, which is only slightly higher than Zollweg's value of 3.0 A. For the radiation efficiency, defined by Eqs. (48) and (49), we obtain $W=0.656$, and the parameter ξ has the value 0.956 which is fairly close to unity. The temperature profiles are compared in Table II. Of course, our temperature is independent of the axial coordinate, but Zollweg's varies somewhat along the axis. Therefore, we have chosen a position halfway along the electrodes of Zollweg's lamp, where we compare our results with his. It can be seen that our EH model predicts temperatures that are 3%–4% lower in the center of the tube and somewhat higher ones closer to the tube wall. On the whole, our temperature profile would seem to be somewhat flatter in the central portion of the tube. Outside this central region its gradient is slightly steeper than Zollweg's.

Clearly, a complete agreement between Zollweg's results and ours cannot be expected, since our radiation model differs to some extent from Zollweg's. Even so, the agreement seems to be quite reasonable. This is all the more surprising, since the convection model shows axial variation, whereas ours does not. For reference purposes we have collected some values pertaining to this case in Table III. The values of the variables are those calculated by our method.

TABLE III. Values pertaining to a case studied by Zollweg.[a] Calculated values are ours.

Physical constants	
a	0.009 m
E	1382 V/m
t_i	54 600 K
t_r	5621 K
t_w	1000 K
t_*	86 000 K
I	3.43 A
P	379.4 W
V	110.6 V
γ	1.2×10^{3} mho/m/K$^{3/4}$
λ_r	0.0661 W/m/K
ω	2.14×10^{18} W K/m^3
Dimensionless constants	
$f(T_i)$	1.55×10^{6}
g_1	6.787
g_2	12.91
g_3	19.74
H	19.7
K	18.8
p	-1
Q_w	4.92
T_i	9.714
T_w	0.178
T_*	15.3
W	0.656
α	1.27×10^{-5}
η	1.575
ξ	0.956
Ω	0.806×10^{9}
$\int_{T_w}^{1}\Lambda(T)dT$	0.506

[a]See Ref. 8.

VII. HIGH RADIATION EFFICIENCY

The example of the previous section led to a value of the radiation parameter ξ close to unity. Inspection of Fig. 4 reveals that, for most values of the parameter η, ξ must be very close to unity for the radiation efficiency to be above 0.5, say. Therefore, a special analysis devoted to this limiting case seems justified. As the asymptotic analysis for $\xi\uparrow1$ is rather technical from a mathematical point of view, we present the details elsewhere.[11,12] However, we shall use and discuss the results here. For $\xi\uparrow1$ the important Eq. (42) can be written

$$B(\xi,\eta)=M\exp[-N/A(\xi,\eta)], \tag{52}$$

$$M=(\eta-1)^{1/2}\Omega^{1/2}\exp(-\tfrac{1}{2}\eta T_i), \tag{53}$$

$$N=T_i\left(\frac{\eta}{2}\right)^{1/2}\int_{T_w}^{1}\Lambda(T)dT, \tag{54}$$

$$B(\xi,\eta)\sim L+\tfrac{1}{2}\ln(L)+c_1(\eta)+\frac{1}{4}\frac{\ln(L)}{L}+\frac{c_2(\eta)}{L}+\cdots, \tag{55}$$

$$A(\xi,\eta)\sim L+\tfrac{1}{2}\ln(L)+c_3(\eta)+\frac{1}{4}\frac{\ln(L)}{L}+\frac{c_4(\eta)}{L}+\cdots, \tag{56}$$

where L is defined by

$$L=\ln[1/(1-\xi)]. \tag{57}$$

The coefficients c_1, c_2, c_3, and c_4 appearing in Eqs. (55) and (56) are listed in Table IV. The dimensionless physical parameters M and N are functions of the gas properties and are fixed for each individual case. The parameter $\eta=t_*/t_i$ is also given. Therefore, Eq. (52) is a seemingly complicated equation for the unknown ξ. It should be noted that the expressions for A and B are asymptotic expansions which apply for $\xi\uparrow1$. The closer ξ is to unity, the better these truncated asymptotic series are.

It is a fairly simple matter to obtain the solution to Eq. (52). This is best achieved iteratively. In the first iteration step we choose $B=M$. Clearly, since the exponential function in Eq. (52) is always less than unity, B can at most be

TABLE IV. Constants used in Eqs.(55), (56), and (62).

η	c_1	c_2	c_3	c_4	c_5	c_6
1.05	−1.8394	1.8789	−0.8888	1.4270	−2.2689	6.0971
1.10	−1.1683	2.2207	−0.2170	1.7682	−1.5654	4.1687
1.15	−0.7833	2.4231	0.1691	1.9696	−1.1497	3.5217
1.20	−0.5145	2.5705	0.4393	2.1156	−0.8517	3.2899
1.25	−0.3088	2.6890	0.6466	2.2325	−0.6183	3.2473
1.30	−0.1428	2.7901	0.8146	2.3318	−0.4257	3.3064
1.35	−0.0038	2.8799	0.9558	2.4195	−0.2614	3.4258
1.40	0.1156	2.9618	1.0776	2.4991	−0.1177	3.5836
1.45	0.2202	3.0381	1.1847	2.5730	0.0103	3.7667
1.50	0.3133	3.1102	1.2805	2.6424	0.1258	3.9673
1.55	0.3971	3.1790	1.3671	2.7085	0.2312	4.1801
1.60	0.4733	3.2454	1.4463	2.7719	0.3283	4.4017
1.65	0.5433	3.3098	1.5194	2.8333	0.4184	4.6296
1.70	0.6079	3.3726	1.5872	2.8930	0.5026	4.8622
1.75	0.6680	3.4341	1.6506	2.9514	0.5816	5.0981
1.80	0.7243	3.4946	1.7102	3.0086	0.6561	5.3366
1.85	0.7771	3.5543	1.7664	3.0649	0.7267	5.5767
1.90	0.8269	3.6132	1.8198	3.1203	0.7938	5.8182
1.95	0.8741	3.6716	1.8705	3.1752	0.8578	6.0604
2.00	0.9189	3.7294	1.9189	3.2294	0.9189	6.3033

equal to M. However, B must also be much larger than unity. This can be seen from Eqs. (55) and (57), since $L \gg 1$. Therefore,

$$1 \ll B \ll M. \tag{58}$$

This shows that the analysis of this section will only work if

$$M \gg 1, \tag{59}$$

or, in other words, if Eq. (59) is not satisfied, we must conclude that ξ cannot be close to unity, and high radiation efficiency is not achieved for the particular parameter setting used.

Proceeding now with our iteration procedure, we invert Eq. (55), which yields

$$\xi \sim 1 - \exp[-B + \tfrac{1}{2}\ln(B) + c_1 + (c_2 - \tfrac{1}{2}c_1)/B + \cdots]. \tag{60}$$

Substituting our initial choice $B = M$ in Eq. (60), we obtain an initial estimate of ξ. Substituting this initial value in Eq. (56), we obtain A, and this in turn yields a new value of B, upon application of Eq. (52). If the values of M and N are such that a solution for ξ close to unity exists, this procedure will converge to that solution. It may be necessary to apply under-relaxation.

We shall illustrate the above procedure by means of the example of the previous section. Referring to the values listed in Table III, we find $M = 10.25$ and $N = 4.362$. Using Table IV, we may find interpolated values for $\eta = 1.575$: $c_1 = 0.4362$, $c_2 = 3.2126$, $c_3 = 1.4077$, and $c_4 = 2.7406$. This provides all the information we need to carry out the iteration procedure described above. In fact, it can be carried out on a simple pocket calculator. For illustrative purposes we list the iterated values in Table V. The final value of $\xi = 0.959$ is very close to the value of $\xi = 0.956$ found before.

TABLE V. Iteration procedure involving Eqs. (52), (56), and (60).

B	ξ	A
10.25	0.9998	11.22
6.948	0.9940	7.951
5.922	0.9833	6.959
5.476	0.9738	6.538
5.260	0.9674	6.338
5.150	0.9636	6.237
5.093	0.9614	6.185
5.064	0.9603	6.159
5.048	0.9596	6.145
5.040	0.9593	6.137
5.036	0.9591	6.134
5.034	0.9590	6.132
5.033	0.9590	6.131
5.032	0.9589	6.130
5.031	0.9589	6.130
5.031	0.9589	6.130

It is shown in Ref. 11 that an asymptotic representation of W can be found that is accurate in the range $0.9 < \xi < 1$,

$$W \sim 1 - 2(\eta - 1)(2/\eta)^{1/2}\{1/[L + \tfrac{1}{2}\ln(L)]\}. \tag{61}$$

Applying this formula for $\xi = 0.959$, we find $W = 0.657$, which is remarkably close to the earlier value of $W = 0.656$. This is probably a fortuitous coincidence. Indeed, in Ref. 11 we found a more complete asymptotic representation of W which gives a less accurate result. Although the extended formula of Ref. 12 is more accurate when ξ is extremely close to unity, the truncated formula Eq. (61) happens to be more accurate when ξ is not so close to unity, let us say $0.9 < \xi < 0.99$.

Next, we shall calculate the current I. It is clear from Eqs. (15) and (41) that we need the value of g_3 first. In Ref. 12 we derived an asymptotic representation of g_3 valid for $\xi \uparrow 1$:

$$g_3 = \tfrac{1}{2}(\eta - 1)^{-1}\{L^2 + L\ln(L) + 2c_5(\eta)L + \tfrac{1}{4}\ln^2(L) + [c_5(\eta) + \tfrac{1}{2}]\ln(L) + c_6(\eta) + \cdots\}, \tag{62}$$

where values of c_5 and c_6 are listed in Table IV. Interpolated values for $\eta = 1.575$ are: $c_5 = 0.2809$ and $c_6 = 4.2904$. It is also shown in Ref. 12 that the parameter functions g_1 and g_2 can be expressed in terms of the functions defined by Eqs. (55) and (56).

$$g_1 = (2/\eta)^{1/2}A(\xi,\eta), \tag{63}$$

$$g_2 = g_1\{\ln[B(\xi,\eta)/(\eta - 1)^{1/2}]\}. \tag{64}$$

Using (57) and the values of Table IV, we can easily find the values of these parameter functions for $\xi = 0.959$: $g_1 = 6.908$, $g_2 = 13.07$, and $g_3 = 18.47$. These values compare well with the ones presented in Table III, which were obtained by a more involved numerical procedure. From Eq. (41) we now obtain $\alpha = 1.16 \times 10^{-5}$. Substituting this value in Eq. (15), we arrive at $I = 3.28$ A. Again, this value is very close to that obtained before (see Table III).

It would seem that we have demonstrated that the asymptotic analysis of this section is very effective when ξ values close to unity can be expected. Satisfaction of condition (59) would seem to be all important.

VIII. THE CASE $\eta=1$

The analysis of the previous sections is less effective when η approaches unity. Fortunately, for $\eta = 1$ the basic equation (25), subject to the boundary conditions for Eq. (29), can be solved analytically:

$$Q=2\ln[1+(1-\xi)Z^2/8], \tag{65}$$

so that it is possible for us to present fully analytical results for this case. Substituting the outer-wall boundary condition (30) in Eq. (65), we have

$$\exp(Q_w/2)\sim\tfrac{1}{8}(1-\xi)HT_i, \tag{66}$$

where the factor 1 appearing in Eq. (65) has been disregarded, since its value is insignificant in comparison with that of the terms retained. Eliminating H from Eqs. (27) and (66), we find

$$\xi=1/\{1+8T_i^{-1}K^{-1}\exp(Q_w/2)\}. \tag{67}$$

Substituting Eq. (65) in Eq. (40) we can derive

$$g_3=4/(1-\xi), \tag{68}$$

so that Eqs. (39) and (66) yield

$$\alpha=[2/(1-\xi)]T_i^{-1}\exp(-T_i-Q_w/2). \tag{69}$$

Equations (15) and (69) produce the following result:

$$I=2^{3/2}\pi a\gamma^{1/2}\lambda_r^{1/2}\lambda_r^{11/8}t_i^{-1/2}(1-\xi)^{-1/2} \times\exp(-\tfrac{1}{2}T_i-\tfrac{1}{4}Q_w), \tag{70}$$

which shows how the total arc current depends upon the system parameters. With $\eta = 1$, Eq. (49) shows that the radiation efficiency is given by Eq. (67).

IX. CONCLUDING REMARKS

In this paper we have shown that the classical Elenbaas–Heller equation for a radiating wall-stabilized high-pressure gas-discharge arc can be treated almost totally by analytical means, notwithstanding its severe nonlinearities. Those cases that are of practical importance, viz. those that involve a high radiation efficiency, admit a full analytical treatment up to a simple numerical iteration procedure, which can be carried out on a regular programmable pocket calculator.

To make sure that the high-efficiency regime applies, the value of the dimensionless parameter M [Eq. (53)] must be determined first. If M is large, the lamp operates in this particular regime. In the example discussed in this paper a value of M around 10 proved to be sufficiently large. The next step is the determination of the parameter ξ, which is done iteratively. Choosing $B = M$ initially, we calculate ξ by means of Eq. (60). Next we calculate the parameter A using Eq. (56), and this in turn enables us to find a new value of B through Eq. (52). This brings us back to Eq. (60) for a new value of ξ, and so on, until convergence is achieved. This process can be carried out on the above-mentioned pocket calculator.

If M is not large, high efficiency is not achieved. We are then forced to use Eq. (42) in an iterative process for the calculation of ξ. In principle, this could also be done by hand, using the graphical representations of the functions g_1 and g_2. Alternatively, the iteration process could be executed by carrying out repeated numerical integrations of Eq. (25) for the various iteration values of ξ. Each separate integration produces values of g_1, g_2, and g_3. This requires a low-powered table-top computer.

Once ξ is known, all pertinent lamp parameters, such as the current [Eq. (45)], the electric field [Eq. (46)], the power [Eq. (47)], and the radiation efficiency [Eqs. (48) and (61)] can be determined through direct computation. Clearly, the whole analysis revolves around the parameter ξ. Yet, this is the most elusive parameter of all. It is difficult to attach a direct physical meaning to it. In any case, it is impossible to express it explicitly in terms of known physical quantities. It is defined implicitly in terms of these through Eq. (42), or, in the case of high efficiency, in terms of the iterative process defined above. The closest we can come to a physical definition of ξ is through Eq. (27). Referring to Eq. (13), we see that ξ is related to the ratio of radiated energy and energy dissipated internally. Even so, it is not equal to this ratio, which is precisely the efficiency W [Eq. (49)].

The principles underlying the asymptotic techniques will also apply to more complicated problems. This means that the intricate nonlinearities can be dealt with efficiently, even in the case of more complex geometries. What will be needed, when dealing with these more advanced cases, is to find a balance between the analytical and the numerical effort.

Problems that may be suitable candidates for the asymptotic treatment are one-dimensional time-dependent ones. Examples of such problems are given in papers dealing with pulsed arcs.[13–15] Such problems are now usually solved by means of software packages. The asymptotic approach can be expected to lead to a better understanding of the structure of pulsed arcs.

Convective flows may also be treated asymptotically. In a recent study[10] on a free-burning arc, we formulated the boundary-layer equations, which in themselves are asymptotic representations of the full energy and momentum equations. Within this boundary-layer model a further asymptotic characterization of the kind discussed in this paper can be given.

ACKNOWLEDGMENTS

The author is indebted to Dr. J. K. M. Jansen of the Math Department of the Technical University of Eindhoven for a useful suggestion concerning the numerical integration of Eq. (25). Thanks are also due to J. A. J. M. van Vliet of the Philips Lighting Division for his encouragement and useful advice on the model discussed in this paper.

[1] H. K. Kuiken, Appl. Phys. Lett. **58**, 1833 (1991).
[2] W. Elenbaas, *The High Pressure Mercury Vapour Discharge* (North-Holland, Amsterdam, 1951).
[3] V. J. Francis, Philos. Mag. **37**, 433 (1946).
[4] H. Maecker, Z. Phys. **157**, 1 (1959).
[5] H. Goldenberg, Br. J. Appl. Phys. **10**, 47 (1959).
[6] A. M. Whitman and I. M. Cohen, J. Appl. Phys. **45**, 3813 (1974).
[7] V. D. Khait, High Temp. **5**, 899 (1979).
[8] R. J. Zollweg, J. Appl. Phys. **49**, 1077 (1978).
[9] J. J. Lowke, J. Appl. Phys. **50**, 147 (1979).
[10] H. K. Kuiken, J. Appl. Phys. **69**, 2896 (1991).
[11] H. K. Kuiken, J. Eng. Math. (to be published).
[12] H. K. Kuiken, Appl. Math. Lett. (to be published).
[13] C. L. Chalek and R. E. Kinsinger, J. Appl. Phys. **52**, 716 (1981).
[14] J. T. Dakin and T. H. Rautenberg, Jr., J. Appl. Phys. **56**, 118 (1984).
[15] D. M. Rutan and P. G. Mathews, J. Illum. Eng. Soc. **18**, 29 (1989).